Iran J Public Health, Vol. 53, No.10, Oct 2024, pp.2260-2270

Original Article

MiR-21-5p Promotes Osteogenic Differentiation and Calcification of Valvular Interstitial Cells by Targeting *TGFBI* in Calcific Aortic Valve Disease

#Yan Gu [1], ***#Rongjin Chen*** [1], ***Jianxiang Song*** [1], ***Zhan Shi*** [1], ***Jixiang Wu*** [1], ***Huiwen Chang*** [1], ***Conghu Yuan*** [2], ****Woda Shi*** [1], ****Yajun Zhang*** [1]

1. *Department of Cardiothoracic Surgery, The Sixth Affiliated Hospital of Nantong University, Yancheng Third People's Hospital, Yancheng, Jiangsu 224000, China*
2. *Department of Anesthesiology, The Sixth Affiliated Hospital of Nantong University, Yancheng Third People's Hospital, Yancheng, Jiangsu 224000, China*

***Corresponding Authors:** Email: ycsyswd@ntu.edu.cn, ycsyzyj@126.com
# Contributed equally to this work

(Received 11 Feb 2024; accepted 12 Apr 2024)

Abstract

Background: Calcific aortic valve disease (CAVD) is the most common heart relating disease with high morbidity and mortality, especially in elderly population. While extensive investigations have been devoted to the study of mechanistic pathways related to CAVD, the key factors and mechanisms mediating valve mineralization remain unclear. The aim of this study is to investigate the role of mirnas and their downstream targets in CAVD disease progression. A previous recent multi-omics study suggested a novel CAVD molecular interaction network contained *miR-21-5p*.

Methods: CAV and their pair-matched adjacent normal tissues were obtained from 15 patients pathologically diagnosed as CAVD and admitted in Yancheng Third People's Hospital (The Sixth Affiliated Hospital of Nantong University) from 2019-2021. RT-qPCR was utilized for detection of *miR-21-5p* and related protein expression levels to confirm the related factors in CAVD progression. Western blotting was applied to strengthen the results of RT-qPCR and confirm osteogenic differentiation of VICs via biomarker detection. The staining of alkaline phosphatase (ALP) and alizarin red was performed to assess the degree of VIC mineralization.

Results: We found that *miR-21-5p* was remarkably increased ($P<0.0001$) in calcified aortic valves (AVs) whereas *TGFBI* was diminished ($P<0.01$) in CAVD samples compared to the paired normal tissues from CAVD patients. Additionally, *TGFBI* was targeted by *miR-21-5p*. Furthermore, overexpressing *TGFBI* could block VIC osteogenic differentiation mediated by *miR-21-5p*. To sum up, *miR-21-5p* promotes VIC osteogenic differentiation and calcification via *TGFBI* in CAVD progression.

Conclusion: Our work might bring a sight on underlying mechanisms of CAVD progression and provide a possible therapeutic target for diagnosis and treatment.

Keywords: Osteogenic differentiation; Valvular interstitial cells; Calcific aortic valve disease

Introduction

Calcific aortic valve disease (CAVD) is the most prevalent heart related disease in aging population worldwide with high morbidity and mortality (1), characterized by fibro-calcific leaflet remodeling process that results in from mild to severe aortic valve (AV) sclerosis, and finally leads to lethal AV stenosis (2). To date, there is no effective medical therapeutics available to prevent, halt or even reverse the calcification process in aortic valve leaflets (3). Moreover, the tempt to screen present conventional cardiovascular drugs against CAVD failed in numbers of clinical trials. They could not neither influence disease progression nor reduce adverse outcomes (3). Therefore, in the past decades, intensive research efforts were involved in clarifying the mechanisms of CAVD disease progression and further identifying novel therapeutic targets (4-6). However, the underlying pathophysiological pathways mediating valve mineralization are still incompletely understood.

Valvular interstitial cells (VICs), the main cellular component of the aortic valve, are currently suggested as a plastic cell population. In normal valves, they are responsible for matrix integrity maintenance and compartmentalization (7). But under pathological stimuli, VICs undergo myofibroblast-like cells differentiation and even a subpopulation of VICs displays osteoblastic phenotype which promote initiation of the calcification process of aortic valves (8). Although increasing evidence indicated that a diverse spectrum of cell-dependent mechanisms converges to modulate valvular calcium load, VICs osteogenic differentiation is implicated as the pivotal pathological features in CAVD. However, due to the high heterogeneity of VICs, the key factors and corresponsive mechanisms involving in the VICs differentiation towards mineralization remain to be delineated.

MiRNAs are short non-coding RNAs modulating gene expression by post-transcription manner in many biological processes. In the past few years, the important roles of miRNAs in diagnosis and treatment of cardiovascular diseases, including atherosclerosis, hear failure, cardiac hypertrophy and so on, were revealed in numerous research (9-11). In particular, *miR-21-5p* has been recently validated its role in chronic heart failure (12) and atherosclerosis (13). Additionally, *miR-21-5p* was identified as key factor in pathological mechanism of temporomandibular joint osteoarthritis mediated by its action on extracellular matrix degradation and angiogenesis (14). Furthermore, recent study on multi-omics analysis of CAVD identified a novel 3D network linking the input molecules contained *TGFBI* and *miR-21-5p* (15). Moreover, *miR-21-5p* was demonstrated to target *TGFBI* to induce cell proliferation in non-small cell lung cancer (16) and promote pyroptosis in colorectal cancer (17). Therefore, we speculated that *miR-21-5p* could regulate pathological progression of CAVD via targeting *TGFBI* by regulating VICs osteogenic differentiation.

We validated dysregulation of *miR-21-5p* in CAVD and its associated target *TGFBI* involving in aortic valve mineralization.

Methods

Ethics Statement

This study involving humans complied with the Declaration of Helsinki and was approved by the Ethical Committee of Yancheng Third People's Hospital (The Sixth Affiliated Hospital of Nantong University) and informed consents were obtained from each human donors or the guardians. The number of approval was LS2021024.

Collection of clinical calcific aortic valve samples

The Calcific aortic valves and their pair-matched adjacent normal tissues were obtained from 15 patients pathologically diagnosed as CAVD and admitted in Yancheng Third People's Hospital (The Sixth Affiliated Hospital of Nantong University) from June 2019 to December 2021 (Table 1). These patients consisted of 9 males and 6 females. None of them had congenital malformation of heart valves or rheumatic valvular disease.

Table 1: Patient profiles

Variables	*CAVD(n=15)*	*Control(n=10)*	*P Value*
Age, yr	63.13±8.45	59.90±11.37	0.431
Sex (male/female)	9/6	7/3	0.932
Pre-op EF(%)	57.13±6.91	53.50±9.42	0.249
BMI, kg/m²	25.87±2.03	24.80±2.62	0.659
NYHA classification, n			0.934
< III class	7	4	
≥III class	8	6	
Medical history, n			
Hypertension	8	9	0.137
Diabetes mellitus	5	4	0.932

CAVD, calcific aortic valve disease; Pre-op EF, preoperative ejection fraction; BMI, body mass index; NYHA, New York Heart Association

Extraction of Valve Interstitial Cells (VICs)

To isolate human aortic VICs, tissue samples were obtained from aforementioned patients with acute aortic dissection. A modified isolation procedures of primary VICs were used as described previously (18). Briefly, after washing with phosphate-buffered saline (PBS), the valve leaflets were gently scraped with a blade at the surface to remove endothelial cells. Then, the leaflets were cut into pieces and digested with 2 mg/mL type I collagenase (Sigma-Aldrich) for 8 h at 37◦C in a shaker. The cell suspension was filtered through a mesh screen and subsequently centrifuged. Primary VICs were obtained and maintained in high glucose Dulbecco's modified Eagle's medium (DMEM) containing 10% fetal bovine serum (FBS, Gibico) and Penicilin-Stretomycin. Cells at passages from 3 to 5 were used for all experiments.

Induction of osteoblasts differentiation

Osteogenic differentiation was induced by following procedures according to the previous study (19) with modifications. Briefly, VICs were seeded in 24-well plates and incubate with osteogenic medium (DMEM supplemented with 500 ng/mL recombinant human bone morphogenetic protein-2 (BMP2), 10% FBS, 50 μg/mL ascorbic acid, 10 mM β-glycerophosphate, 100nM dexamethasone). The culture medium was changed every 3 days for 2 weeks.

Cell transient transfection

MiR-21-5p level in VICs were upregulated and downregulated by transfected with the mimic and inhibitor, respectively. And *TGFBI* protein was overexpressed by plasmid transfection. Briefly, cells were seeded in 6-well plates. When the cell achieve 80% confluence, they were individually transfected with 50nM *miR-21-5p* mimic (5-UAGCUUAUCAGACUGAUGUUGA-3), 50 nM *miR-21-5p* inhibitor (5-UAGCUUAUCAGACUGAUGUUGAUGA-3), 50 nM negative control (NC) mimics (5-AGCGUGCCUGAGCAUAGGUGAU-3), NC inhibitors (5-AUGAGCAAUCCACUGCCUGGCA-3), overexpressed (oe)-NC plasmid and oe-*TGFBI* plasmid alone or in combination in OPTI-MEM reduced serum medium (Thermofisher, USA) using lipofectamine 3000 (Thermofisher, USA). The vectors including pcDNA3.1 (overexpression

plasmid) and pGL3-Firefly-Renilla (Dual Luciferase Reporter Gene vector) were purchased from Fenghui Biotechnology Co., Ltd. (FH1215, Changsha, Hunan, China) and Promega (USA), respectively.

Relative RNA level determination by real-time quantitative polymerase Chain Reaction (RT-qPCR)

Total RNA was extracted from cells (24 h after transfection) and tissues using TRIzol (Invitrogen, Carlsbad, CA, United States) and reverse transcribed into complementary DNA (cDNA) according to the manufacturer's protocol (4427975, Applied Biosystems, United States). Primers for *miR-21-5p* (Table 2) were synthesized by GenePharma Co., Ltd (Shanghai, China). Then the assays were performed and analyzed by Bio-RAD CFX96 Real-time System (Bio-RAD, USA). Data were normalized to the internal reference genes *U6* and *GAPDH* for miRNA and mRNA, respectively. The relative transcription level of the target gene was calculated by $2^{-\Delta\Delta Ct}$ method (20). The primers used in this study are listed in Table 2.

Table 2: Primer sequences used for real-time quantitative polymerase chain reaction (RT-qPCR)

Genes		***Primer sequences(5'-3')***
BMP-2	Forward	GGGAGAAGGAGGAGGCAAAG
	Reverse	GAAGCAGCAACGCTAGAAGACA
Osteocalcin	Forward	GAGGGCAATAAGGTAGTGAACAGAC
	Reverse	AATAGTGATACCGTAGATGCGTTTG
TGFBI	Forward	GGTGATGAAATCCTGGTTAGCG
	Reverse	TCGTTCTTGTGGTCGGTTGG
miR-21-5p	Forward	GCGCGTAGCTTATCAGACTGA
	Reverse	AGTGCAGGGTCCGAGGTATT
U6	Forward	CCT GCT TCG GCA GCACA
	Reverse	AAC GCT TCA CGA ATT TGC GT
GAPDH	Forward	GCA AGA GAG AGG CCC TCA G
	Reverse	TGT GAG GGA GAT GCT CAG TG

Western Bolt Analysis

Total proteins were extracted from tissues or cells (48 h after transfection) using ice-cold RIPA lysis buffer (Solarbio, China) and quantified by Pierce BCD Protein Assay kit (Thermofisher, USA). After separation by 10% SDS-PAGE gel, proteins were transferred to a polyvinylidene fluoride (PVDF) membrane, and then blocked with 5% non-fat milk. Subsequently, the PVDF membrane was incubated with the corresponding diluted antibody (Table 3) overnight at 4 ◦C. Then, the membranes were washed and incubated with corresponding secondary antibody (ab205719 or ab205718, abcam, USA). The bands were visualized by BeyoECL Moon kit (Beyotime, China). The protein Maker (PageRuLer Prestained Protein Ladder 10–180 kDa, 26616) was purchased from Thermofisher Company (USA). An exposure apparatus was used to develop proteins, and the quantification of bands was further analyzed by ImageJ software through grayscale module (12, 16).

Table 3: List of primary antibodies

Antibody	*Catalog number*	*company*
Rabbit Anti-Osteocalcin antibody	ab93876	abcam
Rabbit Anti-BMP-2 antibody	ab284387	abcam
Rabbit Anti-*TGFBI* antibody	ab169771	abcam
Mouse Anti-*GAPDH* antibody	ab8245	abcam
Goat anti-Mouse IgG H&L (HRP)	ab205719	abcam
Goat anti-Rabbit IgG H&L (HRP)	ab205718	abcam

Dual Luciferase Reporter Gene Assay

The *TGFBI*-Wild type (*TGFBI*-Wt) cDNA fragments, containing the binding site of miR-21-3p that predicted by TargetScan 7.0 (https://targetscan.org/) and corresponding mutant sequence (*TGFBI*-Mut) were inserted into the pGL3-Firefly-Renilla vector (E1761, Promega Corporation, USA), respectively. VICs were transfected with *miR-21-5p* mimics, *miR-21-5p* inhibitors or corresponding negative control (NC-mimics or NC-inhibitors), and then transfected with indicated dual-luciferase constructs (*TGFBI*-Wt or *TGFBI*-Mut). Luciferase activity was measured by performing Dual Luciferase Reporter Gene Assay Kit (RG027, Beyotime, China) through multiscan spectrum SpectraMax M5 (Molecular Devices, Shanghai, China).

Alizarin Red Staining

Mineral deposition in induced osteoblasts was visualized by Alizarin Red Staining (ARS) based on the previous report with modifications (21). Briefly, differentiated VICs were fixed with precold 95% ethyl alcohol for 15 min and incubation with alizarin red solution for 5 min. Then the cells were eluted with distilled water to remove excessive dye. The dyed cells were mounted after air-drying. The microscope (Carl Zeiss AG, Jena, Germany) was used to observe calcified nodules in VICs after indicated treatments.

Alkaline Phosphatase (ALP) Staining

The ALP activity of differentiated osteoblasts from VICs was detected using the ALP stain kit (P03215, Beyotime, China) according to the manufacturer's instructions. After staining, cells were eluted with distilled water for 2–3 times to terminate the reaction. The microscope (Carl Zeiss AG, Jena, Germany) was used to observe staining in differentiated VICs after indicated treatments.

Statistical Analysis

All measurement data were statistically analyzed with GraphPad Prism 6.0 software and were presented as mean ± standard deviation, with at least three independent experiments. Differences between two groups were compared by unpaired Student's t test, and comparison among multi-sample analysis was perfomed by one-way analysis of variance (ANOVA) and Tukey post hoc test. $P < 0.05$ was considered to be statistically significant.

Results

miR-21-5p was significantly up-regulated in Calcified Aortic Valves (AVs)

The results indicated that *miR-21-5p* was high-expressed in CAVD group compared with control (Fig. 1, $P<0.0001$).

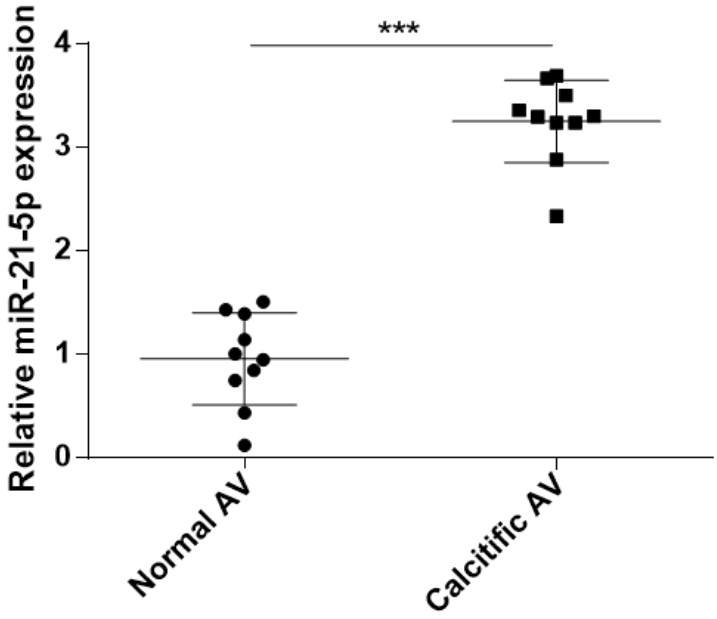

Fig. 1: The expression of *miR-21-5p* is upregulated in calcified AVs. The expression of *miR-21-5p* in tissue samples of calcific aortic valves (n=15) and their pair-matched adjacent normal tissues (n=10) was detected by RT-qPCR. Data are presented as mean±standard deviation and compared using the unpaired Student's *t* test ($P<0.0001$)

miR-21-5p promote osteogenic differentiation and calcification of VICs

To investigate *miR-21-5p* effect on differentiation and calcification of VICs, we first verified the effect of *miR-21-5p* mimics or inhibitors on primary VICs by transfection. *miR-21-5p* mimics and inhibitors could upregulated and downregulated *miR-21-5p* level of isolated primary human aortic VICs from non-calcified tissues, respectively (Fig. 2A). Considering that VICs undergo a phenotype transition towards osteoblasts during CAVD, we then performed assays to confirm whether *miR-21-5p* was involved in osteogenic differentiation and calcification of VICs. As shown in Fig. 2B and 2C, the protein levels of two known osteoblastic differentiation markers (*BMP2* and *osteocalcin*) were remarkably upregulated or downregulated when *miR-21-5p* were overexpressed or knockdown in normal VICs, respectively ($P<0.001$). Additionally, alizarin red staining and ALP measurement results further indicated existence of osteogenic differentiation in VICs. The staining results showed that the number of calcium nodules and ALP activity were increased by *miR-21-5p* mimic but decreased by *miR-21-5p* inhibitor (Fig. 2 D and E). In summary, the results suggested that *miR-21-5p* could enhance VICs osteogenic differentiation and calcification.

miR-21-5p promote Osteogenic differentiation and calcification of VICs by targeting TGFB1 directly

Given that *miR-21-5p* overexpressed in Calcific AVs and associated with VICs osteoblast differentiation, we investigate whether *TGFBI* could reprogram differentiated VICs back to a normal phenotype. As shown in Fig. 4A and 4B, overexpressed *TGFBI* could restore dysregulated *BMP2* and *osteocalcin* to the initial levels in undifferentiated VICs. Furthermore, calcium nodules and ALP activities in *TGFBI* overexpressed groups were significantly decreased compared with the negative control groups (Fig. 4C and 4D). And *TGFBI* overexpression could also inhibit calcium nodules and ALP activities upregulation mediated by *miR-21-5p* mimic transfection.

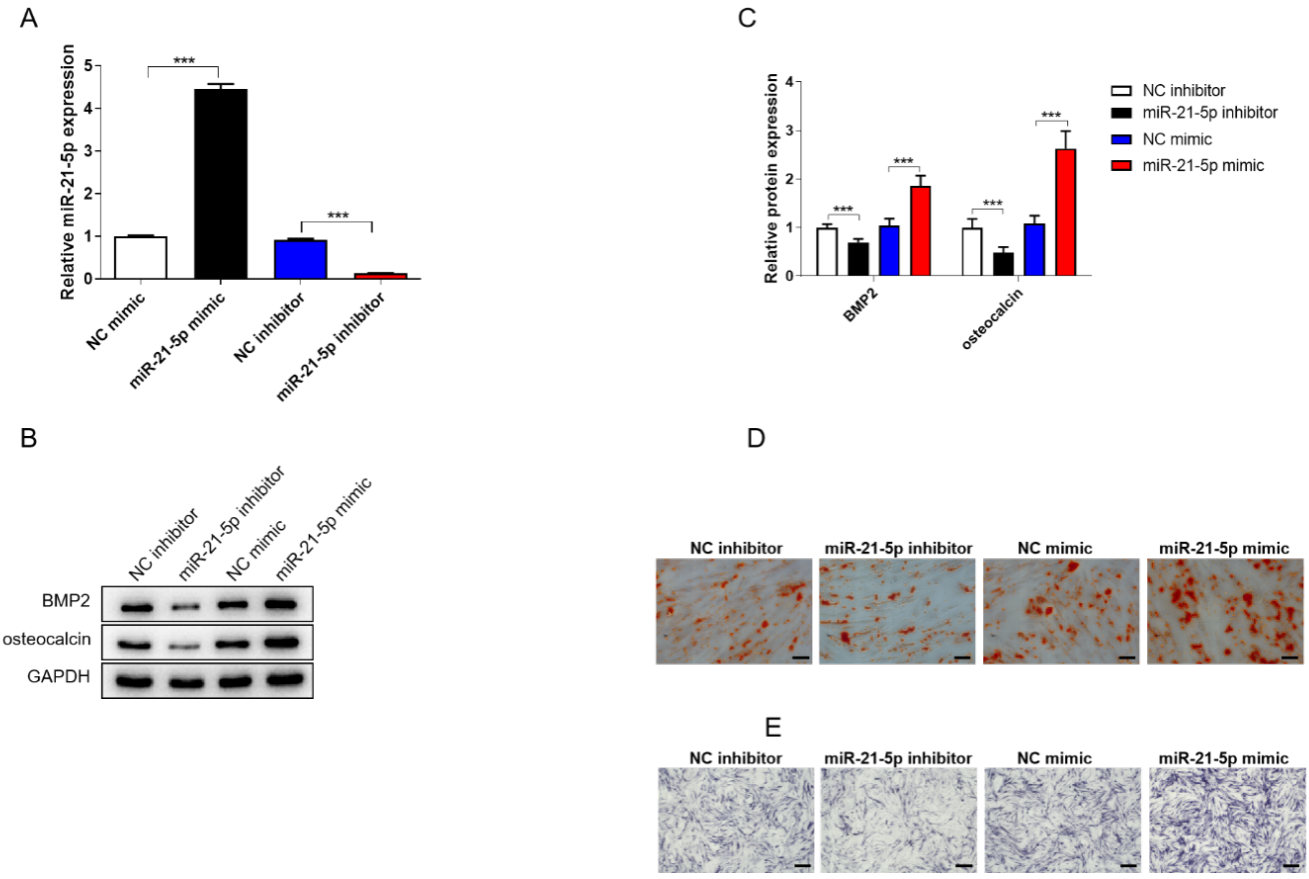

Fig. 2: The level of *miR-21-5p* was possibly correlated with primary VICs differentiation and calcification. (A) *MiR-21-5p* levels were detected by RT-qPCR after primary VICs were transfected with *miR-21-5p* mimic, *miR-21-5p* inhibitor and their corresponding negative controls (miR-NC mimic and inhibitor). (B,C) Representive western blotting images of the expression of *BMP2* and *osteocalcin* in transfected VICs and the grey values of the bands were anaylzed for quantification. (D) Alizarin red staining (200X) of transfected VICs for calcium nudes dectection indicated the undergoing osteogenic transition. (E) ALP staining (200X) of transfected VICs for ALP acvtivites. All the representive images were from three independent experiments for each assay. ***P<0.001. Scale bar=50 μm

TGFBI acted as a CAVD key regulator targeted by *miR-21-5p*

To further validate the role of *TGFBI* in CAVD, immunoblotting and RT-qPCR assays were performed to access *TGFBI* expression differences between calcified and normal leaflet tissues. The results showed that *TGFBI* was remarkably diminished in calcified aortic valves compared with paired normal tissues (P<0.01, Fig. 3A and 3B). We next verified that *TGFBI* expression in VICs regulated by *miR-21-5p* (Fig. 3C and 3D). Moreover, the results of dual luciferase report gene assay demonstrated that *miR-21-5p* could target *TGFBI* by posttranscription regulation through the binding site predicted by Targetscan (Fig. 3E).

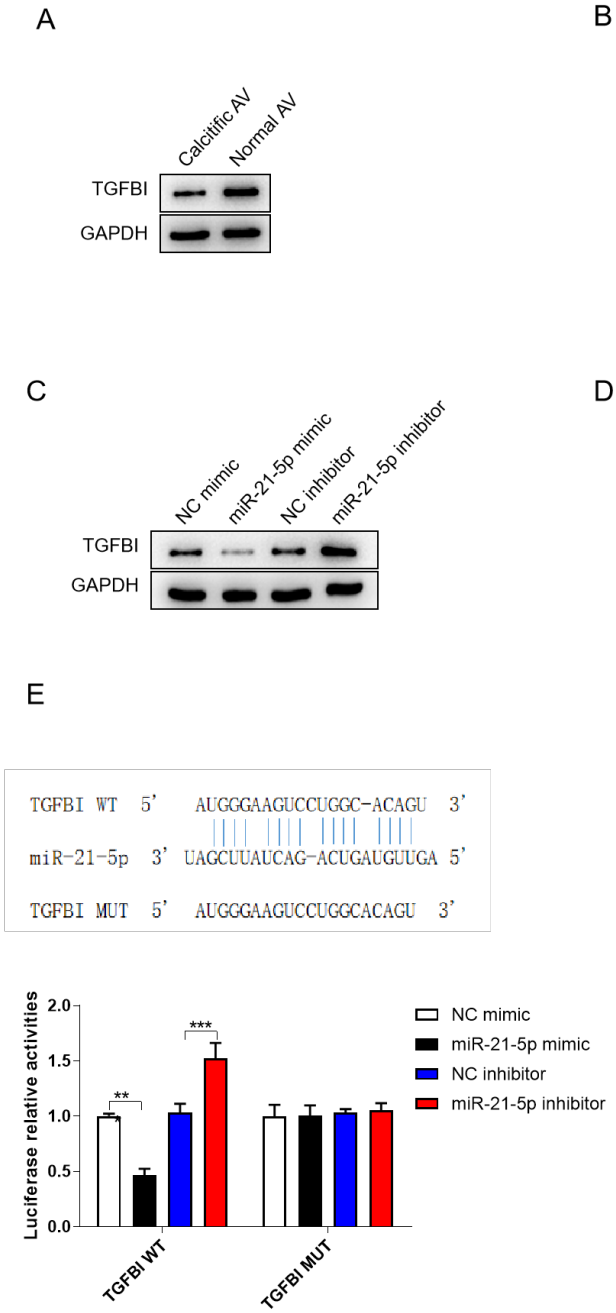

Fig. 3: The expression of *TGFBI* was deregulated in calcified AV compared with paired normal tissues. (A) Representive images of western blotting for *TGFBI* after primary VICs were transfected with *miR-21-5p* mimic, *miR-21-5p* inhibitor and their corresponding negative controls (miR-NC mimic and inhibitor). *GAPDH* was used as loading control. (B) The band grey values were anaylzed by Image J. **P*<0.05,***P*<0.01. (C) Relative mRNA expression levels of *TGFBI* in VICs transfected with different miRNAs as above. **P*<0.05,***P*<0.01. (D) The sequences of binding site of *TGFBI* 3'-UTR with *miR-21-5p* based on the prediction of TargetScan 7.0. (E) Duel-Luciferase reporter assay were performed to verify correlation between *miR-21-5p* and *TGFBI*. The results were expressed as mean±SD based on three independent experiments. ***P*<0.01, ****P*<0.001. WT, wild-type; MUT, mutant

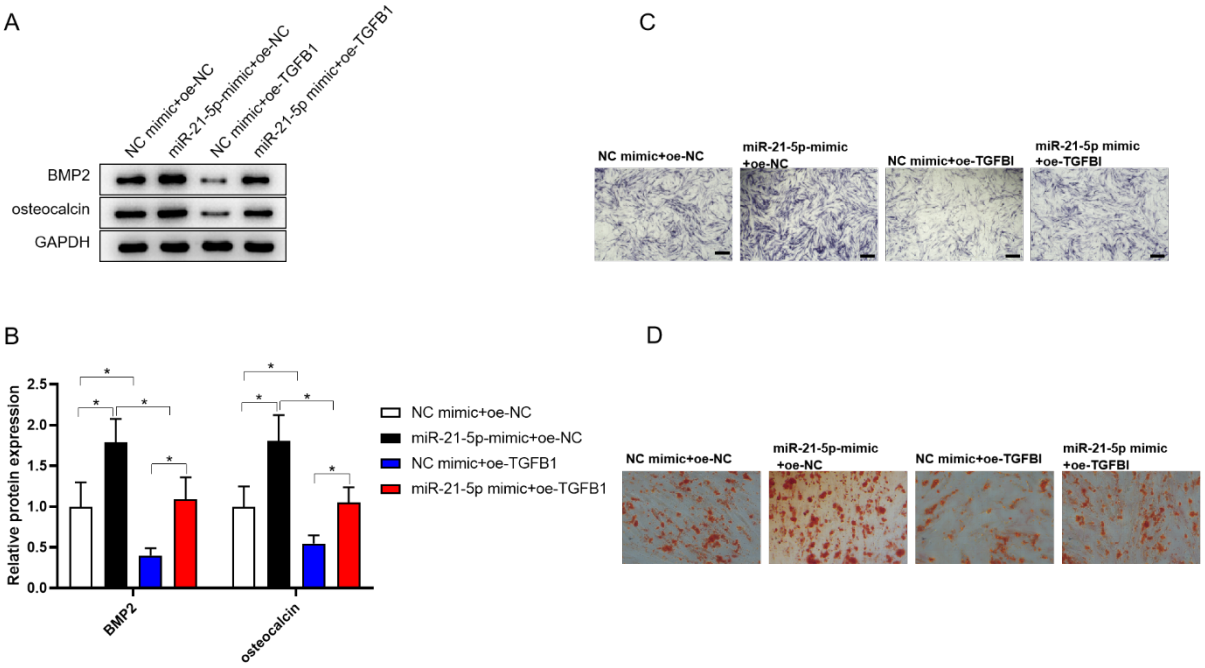

Fig. 4: The osteoblastic differentiation and calcification degree of VICs were promoted by *miR-21-5p* via suppressing *TGFBI* expression. Primary VICs were transfected with miR-NC mimic + oe-NC plasmid; miR-NC mimic+oe-*TGFBI* plasmid; *miR-21-5p* mimic+oe-NC plasmid; and *miR-21-5p* mimic+oe-*TGFBI* plasmid, respectively. (A,B) The biomarker protein levels of osterblatic differentiation (*BMP2* and *osteocalcin*) with different treatment were analyzed by western bloting assay. (C) and (D) Representative staining images for calcium nudes formation and ALP activities were obtained from transfected VICs as above. Data were shown as mean±SD from at least three independent experiments. **P* <0.05, ***P*<0.01, ****P*<0.001. Scale bar=50 μm

Discussion

CAVD is a prevalent disease in aging population and even now no effective drug therapy is available in clinics. Although it is increasingly apparent that multifaceted mechanisms are intricated linked to calcific aortic valve disease pathogenesis, VIC differentiation and possible cross-talks of myofibroblastic and osteogenic transition are considered as vital features of CAVD progression and are further highlighted by numerous studies (5,7,23,24). And recent omics-based studies on normal vs. CAVD tissues built molecular interaction networks and the key factors and disease association were identified (22,25). Previous studies have found *MiR-21-5p* as a key regulator in chronic heart failure and atherosclerosis (12,13), which implied the role of *miR-21-5p* in cardiovascular diseases. Additionally, *miR-21-5p* has been reported to regulate extracellular matrix degradation and angiogenesis of condylar chondrocytes in temporomandibular joint osteoarthritis, which suggested *miR-21-5p* involving in osteogenic pathologies. Based on the study of integrative multi-omics analysis, Heuschkel and her colleagues (15) revealed a novel molecular CAVD network contained *miR-21-5p* and *TGFBI* linked to the formation of amyloid-like structures. However, more evidence remain to obtain directly from clinical samples to further strengthen the associations based on the multi-omics approach. Therefore, in this study, we validated *miR-21-5p* dysregulation in calcified valves from clinic samples. We found that the expression of *miR-21-5p*

was apparently enhanced in calcified aortic valve tissues compared to the paired normal tissues from CAVD patients. Additionally, the results showed that *mi*R-*21-5p* could promote VICs differentiation towards the osteoblastic phenotype which was characterized by upregulation of biomarker protein levels (*BMP*-2 and *osteocalcin*), calcium nude number and ALP activities.

Transforming growth factor-beta (TGF-β) signaling has fundamental roles in both skeletal development and postnatal bone homeostasis. *TGFBI* in TGF-β signaling was found downregulated in bone marrow-derived human mesenchymal stem/stromal cells (hMSCs) (26). Furthermore, it has been implied possible association of *TGFBI* and CAVD by previous multi-omics study. Accordingly, it is necessary to verify whether *TGFBI* involved in the regulaiton of VICs osteogenic transition during CAVD progression. Based on that, we first validated that *TGFBI* was remarkably downregulated in the calcified AVs of CAVD patients compared to the normal ones, which indicated that *TGFBI* indeed involved in the aortic valve mineralization progression. Secondly, we confirmed that overexpressing *TGFBI* could block the process of VICs calcification. Then we also found that *mi*R-*21-5p* regulated the level of *TGFBI* in VICs and affected VICs osteogenic differentiation. Previous studies have demonstrated that *mi*R-*21-5p* could bind 3'UTR of *TGFBI* in colorectal cancer cells and non-small cancer cells (16,17). Therefore, we further detected binding efficiency of the predicted binding site of *mi*R-*21-5p* on *TGFBI* which was different from reported sequences. The results showed that *mi*R-*21-5p* could target *TGFBI* to accelerate osteogenic differentiation of VICs, whereas *TGFBI* overexpression blocked the effect of *mi*R-*21-5p* and halt the calcification progression mediated by *mi*R-*21-5p* upregulation.

Our study for the first time demonstrated that *mi*R-*21-5p* targete *TGFBI* and participate in the progression of AV pathological calcification. However, there are still some limitations in this study, which failed to study the effect of *mi*R-*21-5p*/*TGFBI* on CAVD in animals. Secondly, the potential downstream molecules and signaling pathways involved in the regulation of CAVD progression by *mi*R-*21-5p*/*TGFBI* axis have not been further investigated. Further exploration of this study could help to fully realize the potential role of *mi*R-*21-5p*/*TGFBI* in CAVD.

Conclusion

Our findings revealed potential mechanisms of AV mineralization, and indicating that *mi*R-*21-5p* and its target *TGFBI* are essential factors involved in VIC osteogenic differentiation in the pathological calcification progression of AVs.

Journalism Ethics considerations

Ethical issues (Including plagiarism, informed consent, misconduct, data fabrication and/or falsification, double publication and/or submission, redundancy, etc.) have been completely observed by the authors.

Acknowledgements

This research was supported by Foundation of the Six Affiliated Hospital of Nantong University.

Conflict of Interest

The authors declare that there is no conflict of interest.

References

1. Nkomo VT, Gardin JM, Skelton TN, Gottdiener JS, Scott CG, Enriquez-Sarano M (2006). Burden of valvular heart diseases: a population-based study. *Lancet*, 368(9540):1005-11.
2. Kraler S, Blaser MC, Aikawa E, Camici GG, Lüscher TF (2022). Calcific aortic valve disease: from molecular and cellular mechanisms to medical therapy. *Eur Heart J*, 43(7):683-697.
3. Alushi B, Curini L, Christopher MR, et al (2020). Calcific Aortic Valve Disease-Natural History and Future Therapeutic Strategies. *Front*

Pharmacol, 11:685.
4. Mathieu P, Boulanger MC (2014). Basic Mechanisms of Calcific Aortic Valve Disease. *Can J Cardiol*, 30(9):982-93.
5. Ma X, Zhao D, Yuan P, et al (2020). Endothelial-to-Mesenchymal Transition in Calcific Aortic Valve Disease. *Acta Cardiol Sin*, 36(3):183-194.
6. Myasoedova VA, Ravani AL, Frigerio B, et al (2018). Novel pharmacological targets for calcific aortic valve disease: *Prevention and Treatments*. *Pharmacol Res*, 136:74-82.
7. Rutkovskiy A, Malashicheva A, Sullivan G, et al (2017). Valve Interstitial Cells: The Key to Understanding the Pathophysiology of Heart Valve Calcification. *J Am Heart Assoc*, 6(9):e006339.
8. Decano JL, Iwamoto Y, Goto S, et al (2022). A disease-driver population within interstitial cells of human calcific aortic valves identified via single-cell and proteomic profiling. *Cell Rep*, 39(2):110685.
9. Vegter EL, van der Meer P, de Windt LJ, Pinto YM, Voors AA (2016). MicroRNAs in heart failure: from biomarker to target for therapy. *Eur J Heart Fail*, 18(5):457-68.
10. Çakmak HA, Demir M (2020). MicroRNA and Cardiovascular Diseases. *Balkan Med J*, 37: 60–71.
11. Wojciechowska A, Braniewska A, Kozar-Kamińska K (2017). MicroRNA in cardiovascular biology and disease. *Adv Clin Exp Med*, 26(5):865-874.
12. Chen C, Liu S, Cao G, et al (2022). Cardioprotective Effect of Paeonol on Chronic Heart Failure Induced by Doxorubicin via Regulating the *miR-21-5p*/S-Phase Kinase-Associated Protein 2 Axis. *Front Cardiovasc Med*, 9:695004.
13. Ke X, Liao Z, Luo X, et al (2022). Endothelial colony-forming cell-derived exosomal *miR-21-5p* regulates autophagic flux to promote vascular endothelial repair by inhibiting SIPL1A2 in atherosclerosis. *Cell Commun Signal*, 20(1):30.
14. Ma S, Zhang A, Li X, et al (2020). *MiR-21-5p* regulates extracellular matrix degradation and angiogenesis in TMJOA by targeting Spry1. *Arthritis Res Ther*, 22(1):99.
15. Heuschkel MA, Skenteris NT, Hutcheson JD, et al (2020). Integrative Multi-Omics Analysis in Calcific Aortic Valve Disease Reveals a Link to the Formation of Amyloid-Like Deposits. *Cells*, 9(10):2164.
16. Yan L, Ma J, Wang Y, et al (2018). *mi*R-*21-5p* induces cell proliferation by targeting *TGFBI* in non-small cell lung cancer cells. *Exp Ther Med*, 16(6):4655-4663.
17. Jiang R, Chen X, Ge S, et al (2021). *MiR-21-5p* Induces Pyroptosis in Colorectal Cancer via *TGFBI*. *Front Oncol*, 10:610545.
18. Zhang M, Liu X, Zhang X, et al (2014). MicroRNA-30b is a multifunctional regulator of aortic valve interstitial cells. *J Thorac Cardiovasc Surg*, 147(3):1073-1080.e2.
19. Yang L, Zhu X, Ni Y, et al (2020). MicroRNA-34c Inhibits Osteogenic Differentiation and Valvular Interstitial Cell Calcification via STC1-Mediated JNK Pathway in Calcific Aortic Valve Disease. *Front Physiol*, 11:829.
20. Livak KJ, Schmittgen TD (2001). Analysis of relative gene expression data using real-time quantitative PCR and the 2(-Delta Delta C(T)) Method. *Methods*, 25(4):402-8.
21. Liu GX, Ma S, Li Y, et al (2018). Hsa-let-7c controls the committed differentiation of IGF-1-treated mesenchymal stem cells derived from dental pulps by targeting IGF-1R via the MAPK pathways. *Exp Mol Med*, 50(4):1-14.
22. Blaser MC, Kraler S, Lüscher TF, Aikawa E (2021). Multi-Omics Approaches to Define Calcific Aortic Valve Disease Pathogenesis. *Circ Res*, 128(9):1371-1397.
23. Hjortnaes J, Goettsch C, Hutcheson JD, et al (2016). Simulation of early calcific aortic valve disease in a 3D platform: A role for myofibroblast differentiation. *J Mol Cell Cardiol*, 94:13-20.
24. Liu AC, Joag VR, Gotlieb AI (2007). The emerging role of valve interstitial cell phenotypes in regulating heart valve pathobiology. *Am J Pathol*, 171(5):1407-18.
25. Schlotter F, Halu A, Goto S, et al (2018). Spatiotemporal Multi-Omics Mapping Generates a Molecular Atlas of the Aortic Valve and Reveals Networks Driving Disease. *Circulation*, 138(4):377-393.
26. Ruiz M, Toupet K, Maumus M, Rozier P, Jorgensen C, Noël D (2020). *TGFBI* secreted by mesenchymal stromal cells ameliorates osteoarthritis and is detected in extracellular vesicles. *Biomaterials*, 226:119544.